Geothermal Potential of the Umatilla Indian Reservation, Oregon: Evidence from Detailed Geophysical Investigations

Brent Ritzinger[1], Jonathan Glen[1], Jared Peacock[1], Richard Blakely[1], Patrick Mills[2], Lydia Staisch[1], Scott Bennett[1] and Brian Sherrod[3]

[1]U.S. Geological Survey, Menlo Park, CA 94025

[2]Confederated Tribes of the Umatilla Indian Reservation, Pendleton, OR 97801, [3]U.S. Geological Survey, Seattle, WA 98195

Keywords

Geophysics, geothermal, hydrothermal, hot springs, faulting, structure, seismic reflection, magnetotellurics (MT), gravity, magnetics, potential-field modeling

ABSTRACT

Recent geologic and geophysical investigations were undertaken in northeastern Oregon to better assess earthquake hazards in the region and determine relative favorability for geothermal energy development on lands of the Confederated Tribes of the Umatilla Indian Reservation (CTUIR). This work was funded in part by a Bureau of Indian Affairs grant awarded to the CTUIR to identify areas most suitable for further exploration of geothermal resources. Results from this work were utilized as inputs to a geothermal favorability modeling process that led to the identification of target sites for further geothermal investigation. Beyond the geothermal aspect of this project, the region is of great tectonic significance as it marks the intersection of two major physiographic and geophysical features, the Klamath-Blue Mountain lineament (KBL) and Olympic-Wallowa lineament (OWL), inferred to represent major basement boundaries. The Thorn Hollow and Hite faults, which appear to be major linkages between the KBL and OWL, run through the study area.

New aeromagnetic, gravity and magnetotelluric (MT) surveying, along with fault analyses, were conducted as part of this effort. Detailed geophysical exploration resulted in the collection of 1,380 new gravity stations, 34,524-line kilometers of aeromagnetic data (covering 12,524 km^2) and measurements from 36 MT stations. Two-dimensional (2D) forward-modeling was executed along several profiles using gravity and aeromagnetic data, combined with existing geologic mapping and rock property constraints measured from hand samples and outcrops. These models are used to define lithologic contacts in the subsurface in the absence of well logs or borehole data to determine possible geothermal fluid reservoirs, as well as identify major structures that may act as conduits for the upward migration of geothermal fluids.

1. Introduction

Potential-fields (magnetic and gravity fields) are ideally suited for imaging geologic units and structures reflecting lateral variations in rock density and magnetic properties (magnetic susceptibility and remanent magnetization). Such contrasts may derive from a variety of causes, such as facies changes within a single rock unit, contacts between distinct rock units or changes across geologic structures like faults and folds. These lateral geologic discontinuities result in variations, or anomalies, in potential-field measurements, which relate to the shape, depth and rock-properties of the source rocks. Potential-field methods are effective in resolving the origin of sources and their geometries, particularly when combined with other geologic and geophysical data, and provide an ideal tool in mapping and modeling subsurface geology and structures.

Potential-field methods are useful in geothermal settings, as they can resolve structural features, such as contacts, faults and fracture zones that may play a significant role in transmitting geothermal fluids. A potential-field approach is particularly useful in the Pacific Northwest, where flows of Miocene Columbia River basalt (CRB) dominate the landscape, obscuring much of the pre-Miocene geology and tectonism. The strong magnetic signature of CRB flows makes shallow structures especially easy to identify, while gravity measurements further facilitate modeling of structures and contacts of sub-CRB sediments and basement, as well as better constraining basin geometries.

The magnetotelluric method (MT) measures the Earth's electrical response to natural time-varying magnetic fields. MT uses induction coils to measure the time-varying magnetic source for frequencies between 1000–0.001 Hz, and electric dipoles to measure the Earth's electrical response. Modeling these data reveals variations in electrical conductivity which may reflect changes in lithology and/or rock-saturating fluids, parameters that may play a vital role in further constraining potential geothermal resources. Abrupt changes in conductivity reflecting changes in lithology may signify the existence of major faults or structures acting as conduits for geothermal fluids. In a geothermal context, strong conductors can be inferred to represent clay-rich rock acting as a cap in a geothermal system or indicate the presence of saline geothermal fluids.

We acquired and analyzed aeromagnetic and gravity data to construct detailed 2D profile models to assess potential geothermal fluid reservoirs and resolve structures responsible for migration of geothermal fluids in the study area. MT data collected for this study were modeled in three-dimensions (3D), revealing conductive anomalies that may reflect reservoirs playing host to saline geothermal fluids or clay-rich cap rock critical to confining geothermal fluids. Data sources include approximately 350 existing gravity stations, 1380 new gravity measurements, 54 hand samples for density and susceptibility measurements, 647 outcrop susceptibility measurements, 56 paleomagnetic core samples from 17 CRB flows for remanent magnetization measurements, 34,524 line-kilometers of new aeromagnetic data and measurements from 36 MT stations.

2. Geologic Setting

The Umatilla Indian Reservation (UIR) is situated in northeastern Oregon, its northwest boundary lying ~3 km east of Pendleton, OR, and ~38 km southeast of the Columbia River. Within its bounds is the confluence of two major crustal-scale geophysical features: the

northeast-trending Klamath Mountains—Blue Mountains lineament (KBL) (Riddihough et al., 1986) and southeast-trending Olympic—Wallowa lineament (OWL) (Raisz, 1945; Hooper and Conrey, 1989; Blakely et al., 2011; McCaffrey et al, 2007). Riddihough et al. (1986) suggest that the KBL represents a pre-Tertiary strike-slip continental margin that has subsequently undergone clockwise rotation. Whether and how the KBL continues to deform remains a question open to debate. McCaffrey et al. (2007), along with further support from Blakely et al. (2011), have presented evidence indicating that the OWL represents the focus of complex deformation catalyzed by rotation of the Pacific Northwest relative to stable North America. The complex faulting in the study area is likely the expression of strain and deformation between the KBL and OWL.

Locally, the OWL is represented by the Wallula Fault zone to the north of the UIR (Reidel et al., 1994 and Blakely et al., 2014), while the KBL is manifest by the Hawtmi fault (Ferns et al., 2006 and Herrera et al., 2017), which runs along the southeastern margin of the Pendleton basin, contiguous with the western foot of the Blue Mountains (Figure 1). The region between the OWL and the mapped terminus of the Hawtmi fault is the setting for several large and numerous smaller-scale faults that likely act as linkages between the OWL and KBL. Larger structures include the ENE-striking Wilahatya fault, which intersects the Hawtmi fault near its previously-mapped northern terminus, as well as the NNE-striking Thorn Hollow, Saddle Hollow and Hite faults, which branch to the north from the Wilahatya fault zone as shown in Figure 1, with the Hite fault off the eastern edge of map (Ferns et al., 2006 and Herrera et al., 2017).

The current stress regime is not well defined, as the region exhibits relatively low crustal velocities (McCaffrey et al., 2007) and few well-constrained historic seismic events. Existing strain data suggests NE compressive forces. However, large crustal structures isolate the study region from available strain data, making it difficult to ascertain how well the data represents strain and strain rates within the study area. Sense of motion along many of these structures is also poorly constrained, but previous work and field observations suggest left-lateral with some sense of oblique motion on the NNE-trending structures in the study area, whereas the ENE-striking Wilahatya fault is likely a high angle normal or possibly reverse fault (Ferns et al., 2006). Ferns et al. (2004) states that well logs in the region indicate that the Wilahatya fault zone is truncated by the Hawtmi fault zone, making it reasonable to infer that the other NNE-trending structures to the east likely post-date displacement along the Wilahatya fault zone.

Much of the Blue Mountains are thought to be underlain by the Wallowa island-arc terrane (e.g., Schwarz et al., 2009 and Vallier, 1998). Eocene to Oligocene volcanic rocks (tuffs and altered granite) and Paleocene to Eocene sedimentary packages (sandstones and shales) of the Herren Formation (generally included as part of the Clarno Formation) are exposed along Birch Creek in the southern portion of the study area (Herrera et al., 2017). The sedimentary packages within this Eocene to Oligocene group represent the most likely host for geothermal fluids in the study region. Local surficial geology is dominated by Miocene CRB flows and quaternary sedimentary basins, which obscure much of the pre-Tertiary geology and structure.

3. Data Collection

Prior to this study, existing geophysical data in the region were sparse and of low resolution and quality. As part of the geothermal assessment efforts, a substantial amount of new geophysical data was collected during summer 2017. A comprehensive ground-based gravity survey was

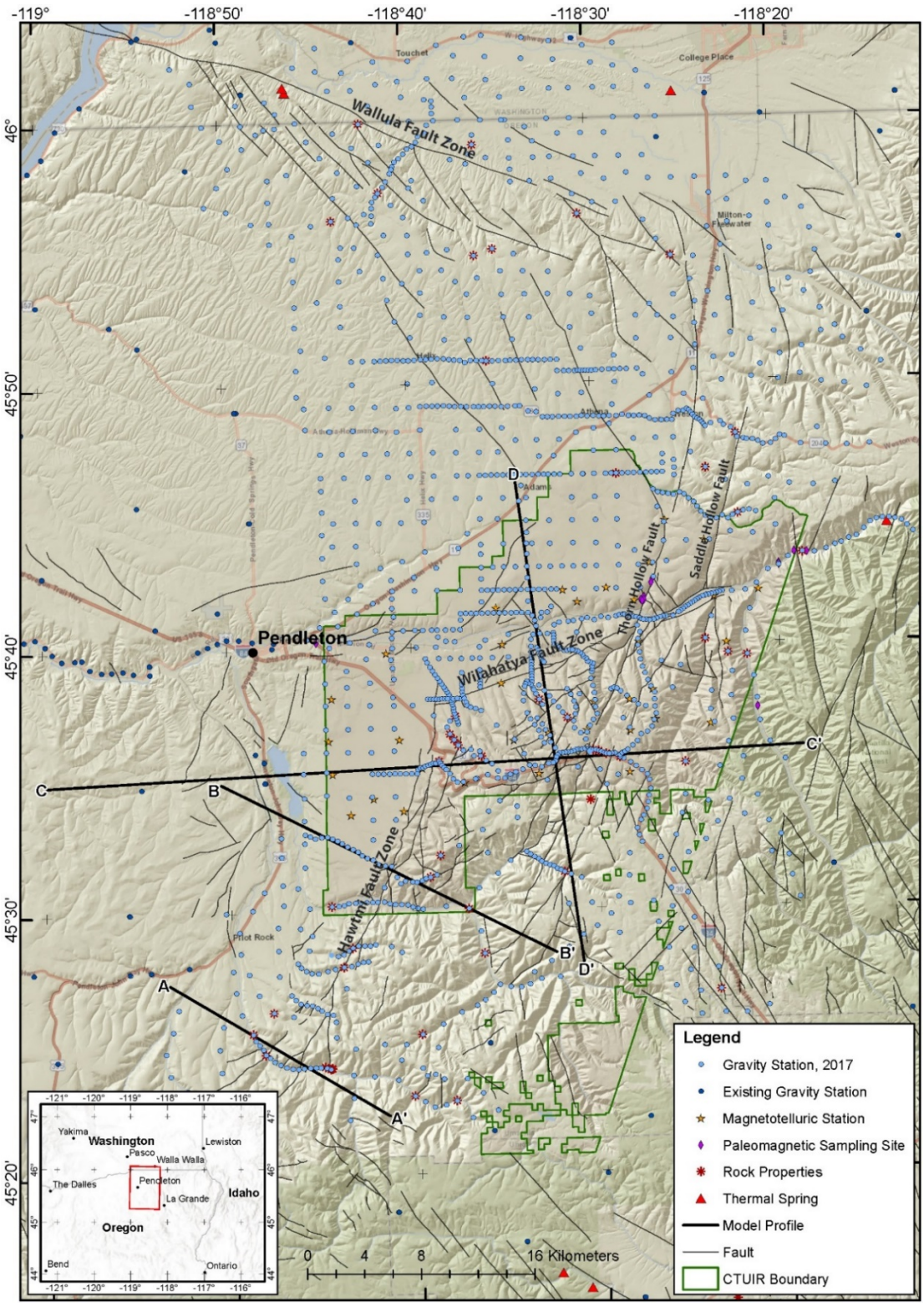

Figure 1. Map of study area illustrating location of gravity stations, rock property data, magnetotelluric stations, paleomagnetic sampling sites and faults (Ferns et al., 2006 and U.S. Geological Survey Quaternary fault database [http://earthquake.usgs.gov/hazards/qfaults]). 2D model profiles are also shown, along with the outline of the UIR.

conducted to fill large holes in existing datasets, whereas detailed gravity profiles were collected along key transects to better constrain important structures. To aid in modeling efforts, magnetic susceptibility measurements were obtained from outcrops encountered during fieldwork, and hand samples were collected for further rock property lab analyses. A high-resolution aeromagnetic survey was flown across the entire study area, while numerous CRB flows were sampled for paleomagnetic analyses to aid in interpretations of the aeromagnetic data. Lastly, a MT survey consisting of 36 stations was conducted in the region in order to create resistivity models that aid in interpreting subsurface geology and identifying important structural features.

3.1 Gravity Data

A database of approximately 350 gravity stations spanning an area of ~110x110 km, covering the entire UIR and study area, was extracted from a public domain dataset, re-reduced and combined with newly acquired gravity stations. The USGS acquired 1380 new gravity stations in the study area (Figure 1), sampled in a grid pattern, at 1600 m intervals when possible, and along detailed (400- to 200-m spacing) profiles. The gravity measurement distribution for this survey was designed to fill gaps in regional gravity coverage, while collecting detailed transects across known, through going faults within the study region. Gravity data were acquired between May and June 2017 with Scintrex CG-5 gravimeters. Base tie measurements were completed at established base stations at the beginning and end of each day to ensure proper meter behavior during the course of fieldwork.

The gravity compilation provides exceptional regional coverage of the UIR Geothermal study area. It also provides detailed control on location of major faults, constrains underlying sediment thickness of the Herren Formation and helps identify variations in crustal composition.

All gravity data were reduced using standard gravity methods (Blakely, 1995) and include the following corrections: (1) earth-tide correction, which accounts for tidal effects of the moon and sun; (2) instrument-drift correction, which compensates for the linear drift of the meter's spring; (3) latitude correction, which corrects for the variation in gravity relative to latitude; (4) free-air correction, which adjusts for the effect of elevation of the gravity measurement relative to sea level; (5) Bouguer correction, which corrects for the gravitational attraction of material between the station and sea level; (6) curvature correction, which amends the Bouguer correction to account for the effect of the curvature of the Earth's surface; (7) terrain correction, which removes the gravitational attraction of all topography within a radial distance of 167 km from each station; and (8) isostatic correction, which accounts for long-wavelength variations in the gravity field caused by deep masses that isostatically support topographic loads.

3.2 Aeromagnetic Survey

34,524-line kilometers of aeromagnetic data were acquired by EDCON-PRJ, Inc., under contract to the U.S. Geological Survey, from June to August 2017. The survey covered 12,524 km^2 encompassing the entire UIR study area. The survey was flown on a surface nominally draped 200 m above terrain, except in areas of rugged terrain. Primary survey lines were directed ~E-W and spaced 400 m apart; ~N-S tie-lines were spaced 4000 m apart. New survey data were merged with existing high-resolution aeromagnetic data collected to the north of the UIR (Blakely et al., 2014).

3.3 Rock Property Data

Accurate potential-field modeling of geology in the subsurface relies on comprehensive knowledge of density and magnetic properties for the units being modeled. Density (dry bulk, grain and saturated bulk density) and magnetic susceptibility measurements were made on hand-samples collected in the field area, representing all exposed lithologies in the field area (Figure 1). Remanent magnetization measurements were made at the USGS on paleomagnetic drill core samples taken from CRB lavas from 17 flows at three locations (Figure 1). Density and magnetic susceptibility measurements were performed at the USGS on hand samples obtained from outcrops.

3.4 Magnetotelluric Data

MT data were collected at 36 stations using induction coils to measure the time-varying magnetic source for frequencies between 1000–0.001 Hz, and electric dipoles to measure the Earth's electrical response. Because the magnetic source field is polarized, orthogonal directions of the fields were measured to get a complete description of the fields. In all measurements collected for this project, induction coils and electric dipoles were aligned with geomagnetic north and east. The data were collected on a repeating schedule of 5 min at 4096 samples/s and 7 hours and 55 minutes at 256 samples over a 20-24 hour period. To convert time series data into the frequency domain and get estimations of impedance tensor, the processing code BIRRP was used (Chave & Thomson, 2004). Simultaneous measurements were used as remote references to reduce noise and bias in the data. MT data analyses are discussed further in section 5.2.

4. Potential-Field Data Interpretation

Gravity and aeromagnetic data were processed and filtered using standard routines available in Oasis Montaj® software. The new gravity data were merged with existing datasets, and isostatic gravity values were gridded using minimum curvature interpolation algorithms at a grid cell size of 400 m. A residual gravity map (Figure 2) was derived by analytically continuing the original isostatic gravity grid upward 1000 m, then subtracting this result from the original grid. This process removes the regional field and emphasizes anomalies arising from density variations in the upper crust, which can aid in identifying shallow crustal faults and contacts.

Airborne measurements of the total magnetic field were reduced to total-field anomalies by subtraction of the International Geomagnetic Reference Field (IGRF). Total-field anomalies then were gridded using minimum curvature interpolation algorithms at a grid cell size of 200 m. Several derivative products were additionally computed to aid in evaluating anomaly sources, including reduced-to-pole (RTP), pseudogravity (magnetic potential), and discrete vertical derivative (residual) transformations (Blakely, 1995). RTP is a method that converts magnetic anomalies to those that would be observed if both magnetization and ambient magnetic field were vertically-oriented, thus effectively centering magnetic anomalies over their sources (Figure 3). The pseudogravity transformation converts a magnetic anomaly into one that would be observed if the magnetic distribution of the body was replaced by an identical density distribution. This process removes edge effects associated with magnetic anomalies and further simplifies analysis of magnetic anomaly data by centering anomalies over their sources. This, in turn, facilitates a more direct comparison with gravity anomalies.

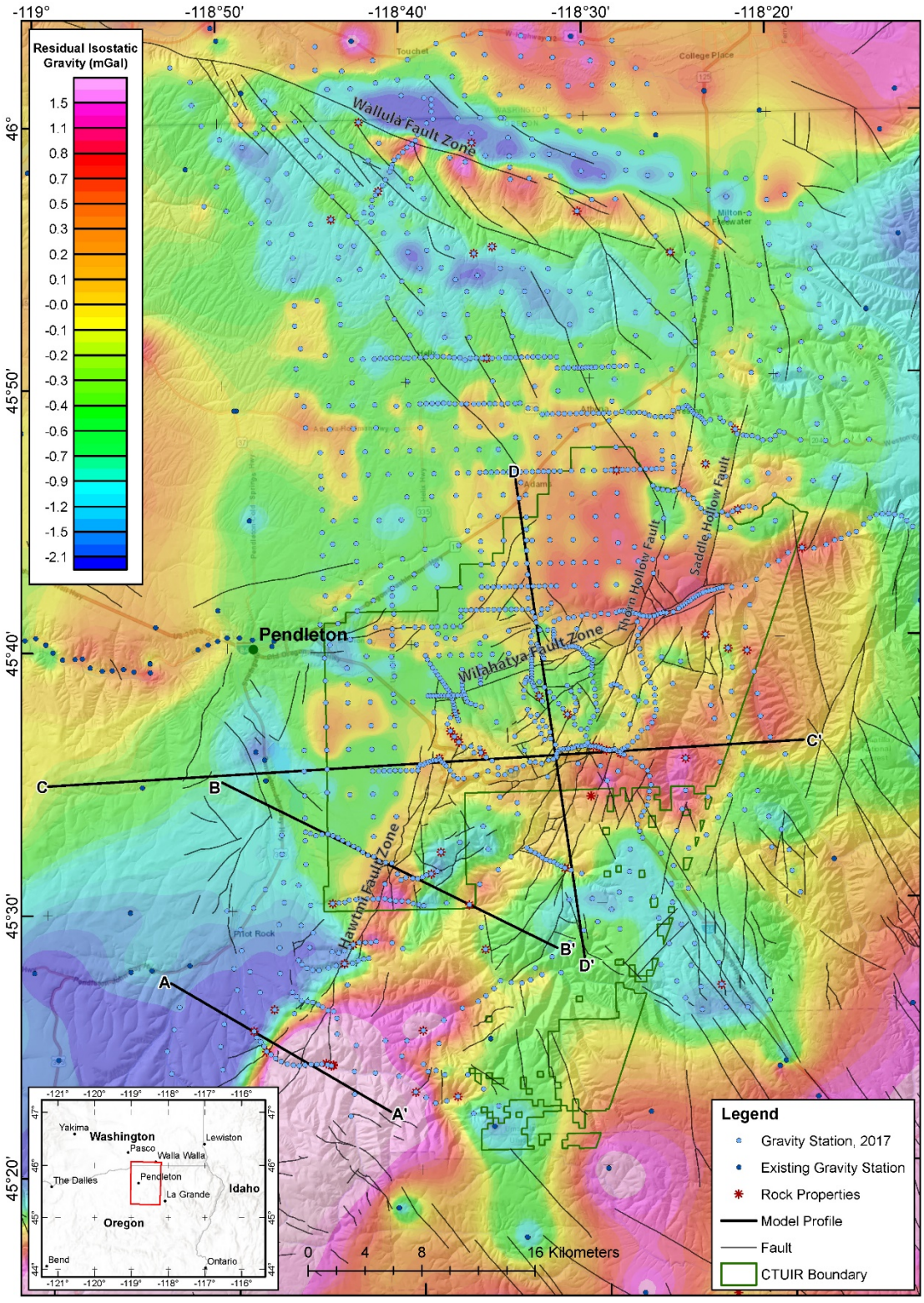

Figure 2 Map of study area showing the residual isostatic gravity grid, as well as gravity stations, rock property locations and faults (Ferns et al., 2006 and U.S. Geological Survey Quaternary fault database [http://earthquake.usgs.gov/hazards/qfaults]).

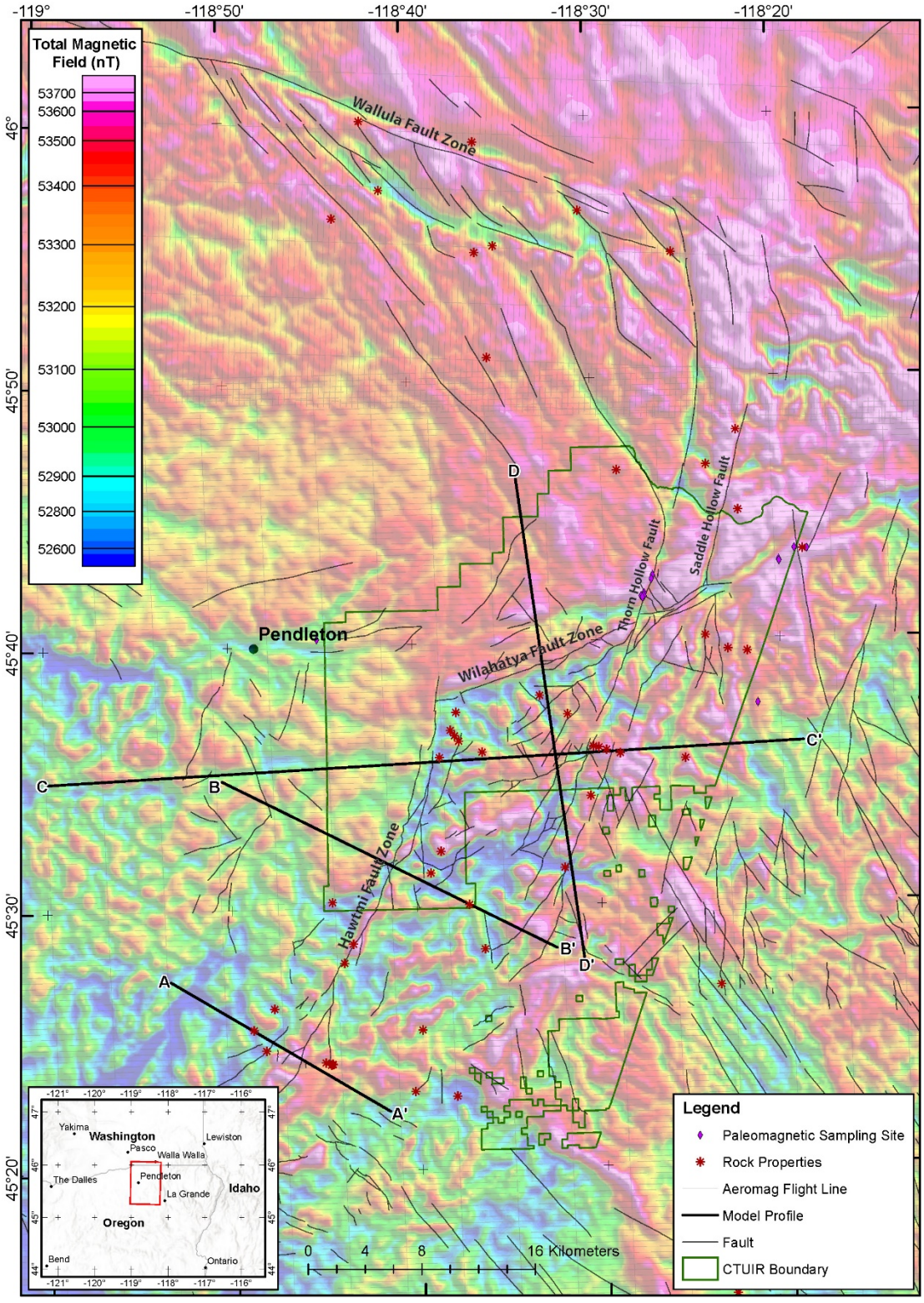

Figure 3. Map of study area showing shaded relief RTP total magnetic field grid, as well as flight lines, paleomagnetic core sample locations, rock property locations and faults (Ferns et al., 2006 and U.S. Geological Survey Quaternary fault database [http://earthquake.usgs.gov/hazards/qfaults]).

A number of other derivative and filtering methods were employed to delineate structures and determine the depth and extent of particular gravity and magnetic anomaly sources. Maximum horizontal gradients (MHG) (Blakely and Simpson, 1986) of isostatic gravity and pseudogravity were calculated to identify abrupt lateral changes in density or magnetization, respectively. Such gradients tend to lie over vertical edges of bodies; dipping contacts shift the determinations slightly in the direction of dip. These gradients often denote contacts between distinct lithologic units and/or structural contacts, aiding in the potential-field modeling process.

Matched filtering (Phillips et al., 2001) of isostatic gravity, pseudogravity and RTP magnetic data was conducted to parse short-wavelength anomalies arising from shallow sources from broad, long-wavelength anomalies that typically arise from sources at greater depths. This procedure is particularly important in the study area because: 1) pre-Tertiary geology is obscured by younger units (CRB flows and sediments) at the surface and 2) anomalies arising from the middle-crust can be difficult to distinguish in the unfiltered maps from those arising from the deeper crust. Matched filtering, in effect, delineates the depth and extent of important source layers thus aiding geologic interpretation and modeling of lithologic units and structures.

5. Modeling

5.1 Potential-Field Modeling

Potential field modeling is implicitly non-unique, so it is vital to integrate all available constraints from all available datasets as part of the modeling process. Joint gravity and magnetic modeling was guided using contacts and structures from geologic maps and, when available, rock properties were prescribed using magnetic and density measurements taken from representative samples and outcrop. Depth slices and cross-sections derived from MT modeling were used to further develop interpretations of potential-field mapping and modeling (e.g., Figure 4). There exists a close correlation between major structures inferred from both MT and potential-field data.

2D potential-field models were developed along four profiles across the study area (one such model, C-C', presented in Figure 4). Modeling was performed using the commercially available GM-SYS® software. This modeling process applies standard forward modeling methods (Talwani et al., 1959 and Blakely and Connard, 1989) that approximate subsurface geologic units with horizontal, tabular prisms that are defined by model blocks in the 2D model cross-sections. The construction of model blocks was informed by and typically remained consistent with available constraints from mapped geologic units. The extents of model blocks were modified through an iterative series of forward and inverse calculations, adjusting density and magnetic properties appropriately, in order to match model anomalies with observed gravity and magnetic anomalies within the limits defined by surface geology, rock property data and MHG, which are useful in estimating the lateral extent of buried sources.

Of the four models, three intersect and are oriented approximately perpendicular to the strike of the NNE-trending Hawtmi fault, while the fourth lies approximately perpendicular to the strike of the ENE-trending Wilahatya fault. The trace of each cross-section was carefully selected to best honor newly collected gravity transect data. Each cross-section includes the modeling of three primary lithologic groups: CRB (normal and reverse-polarity), the underlying generalized sedimentary unit (representing the Herren Formation) and the basement. Rock units within the

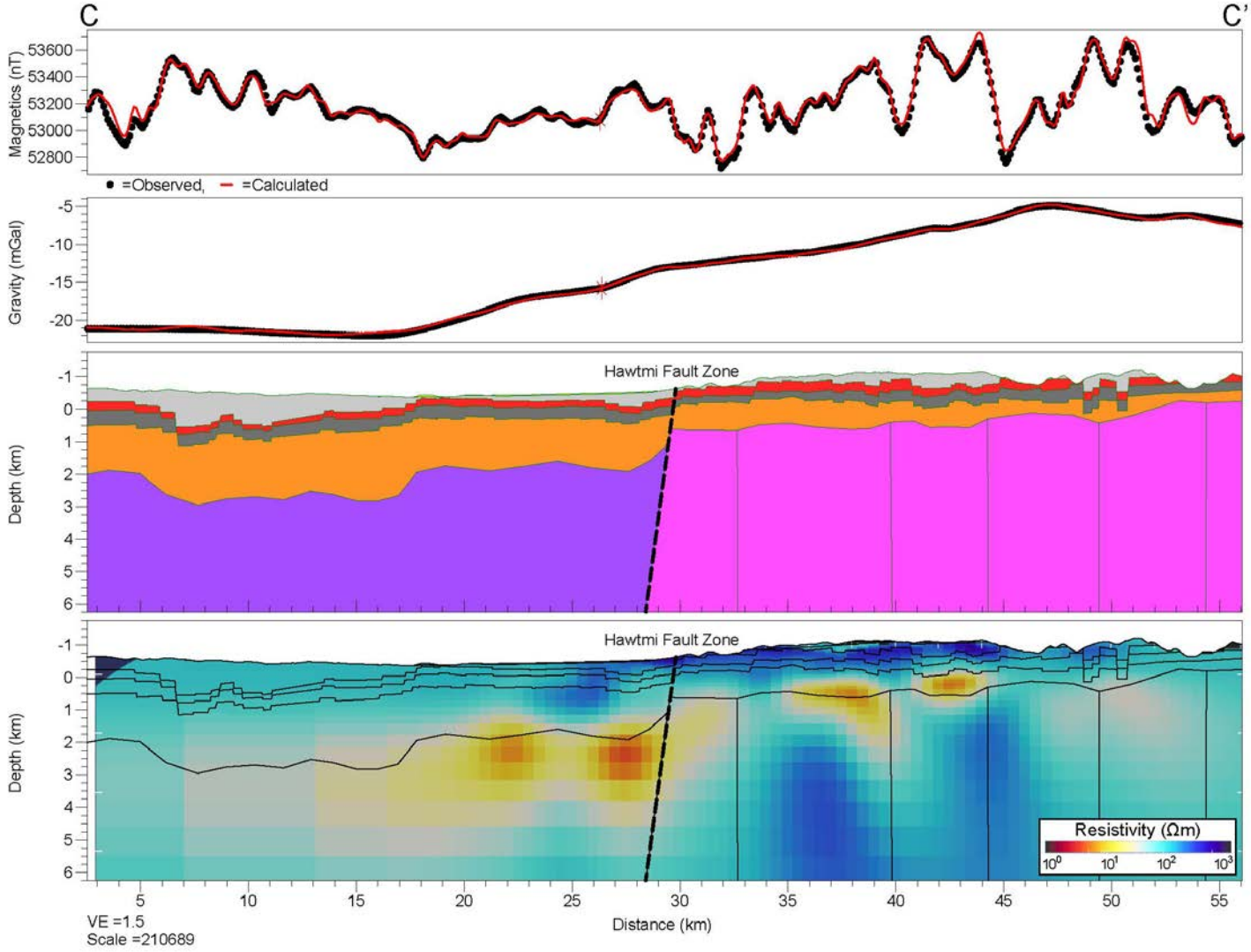

Figure 4. 2D potential-field model along profile C-C' with corresponding MT profile as backdrop in bottom cross-section. Dashed black line indicates the modeled location of the Hawtmi fault. Solid grey and black lines in the bottom two panels, respectively, indicate model block boundaries, but do not necessarily indicate faults. See Table 1 for unit information.

Table 1. Model unit properties for profiles A-A', B-B', C-C' and D-D'.

Model Reference	Representative Unit	Density Range (g/cm^3)	Susceptibility Range (SI)	Magnetization Range (A/m)	Inclination (°)	Declination (°)
	Quaternary Sediments	2.2	0	0	0	0
	N1 CRBG flows	2.7	0.025	3.5	68	0
	R2 CRBG flows	2.7	0.025	4	-43.37	180
	N2 CRBG flows	2.7	0.025	3.5	68	0
	Herren Formation	2.4	0	0	0	0
	Herren or older sediments	2.4	0	0	0	0
	South-central basement	2.78-2.875	0.02-0.046	0	0	0
	Eastern basement	2.67-2.78	0.001-0.04	0	0	0
	Western basement	2.75	0.002-0.04	0	0	0
	Northern basement	2.75	0.04-0.11	0	0	0

model are designated with unique and carefully selected density and magnetic properties based on available rock property data (Table 1 and Rock Property Data section), as well as data derived from a national database (unpublished data, D. Ponce, USGS, 2016), which includes over 19,000 rock property measurements made on a wide variety of lithologies, including those modeled for this study.

Analysis of all profile models illustrate a general trend of depth-to-basement shallowing southward through the Blue Mountains block. This trend is coincident with north to south thinning of sub-CRB sediment from more than a kilometer to several hundred meters. Herren Formation deposits also illustrate west to east thinning, measuring several kilometers thick just west of the Hawtmi fault, reducing to several hundred meters directly east of the fault, and continuing to diminish eastward. The depth to basement increases west of the Blue Mountains, illustrating vertical displacement of hundreds of meters to over a kilometer in some areas along the Hawtmi fault.

5.2 Magnetotelluric Modeling

MT response functions were modeled in three-dimensions (3D) using the code ModEM developed by Egbert & Kelbert (2012) and Kelbert et al. (2014). Input data were edited using the EDI editor in MTpy (Krieger & Peacock, 2014) to remove obvious outliers in the data and suppress bias in the modeling. All data were interpolated onto 23 frequencies in the range of 500-0.001 Hz. The model mesh included topography and was 70 x 91 x 68 cells (north, east, depth) with dimensions of 350 x 350 x 250 km, where spacing within the station area was 500 m increasing by 1.4 away from the station area. The first layer was set to 30 m and increases logarithmically downwards. Inversions were run on NASA's high-end computing capability (HECC) Pleiades super computer, where average run times were on the order of 60 hours.

Multiple conductive and resistive anomalies are present in the preferred 3D electrical resistivity model. A representative depth slice, illustrating a horizontal, planar view through the MT model at 2 km depth, is presented in Figure 5. The general trend is a resistive cover (>200 Ohm-m) that is <1.5 km thick. This layer is interpreted as a combination of alluvium sediment cover and CRB flows. The CRB is underlain by a conductive (< 100 Ohm-m) layer that is variable in thickness (1-4 km) and structure, but has a general plunge to the southwest. This conductive layer coincides with Eocene to Oligocene volcanic rocks and Paleocene to Eocene sedimentary packages of the Herren Formation (Herrera et al., 2017), and the variable structure is related to local and regional tectonics (Figure 5).

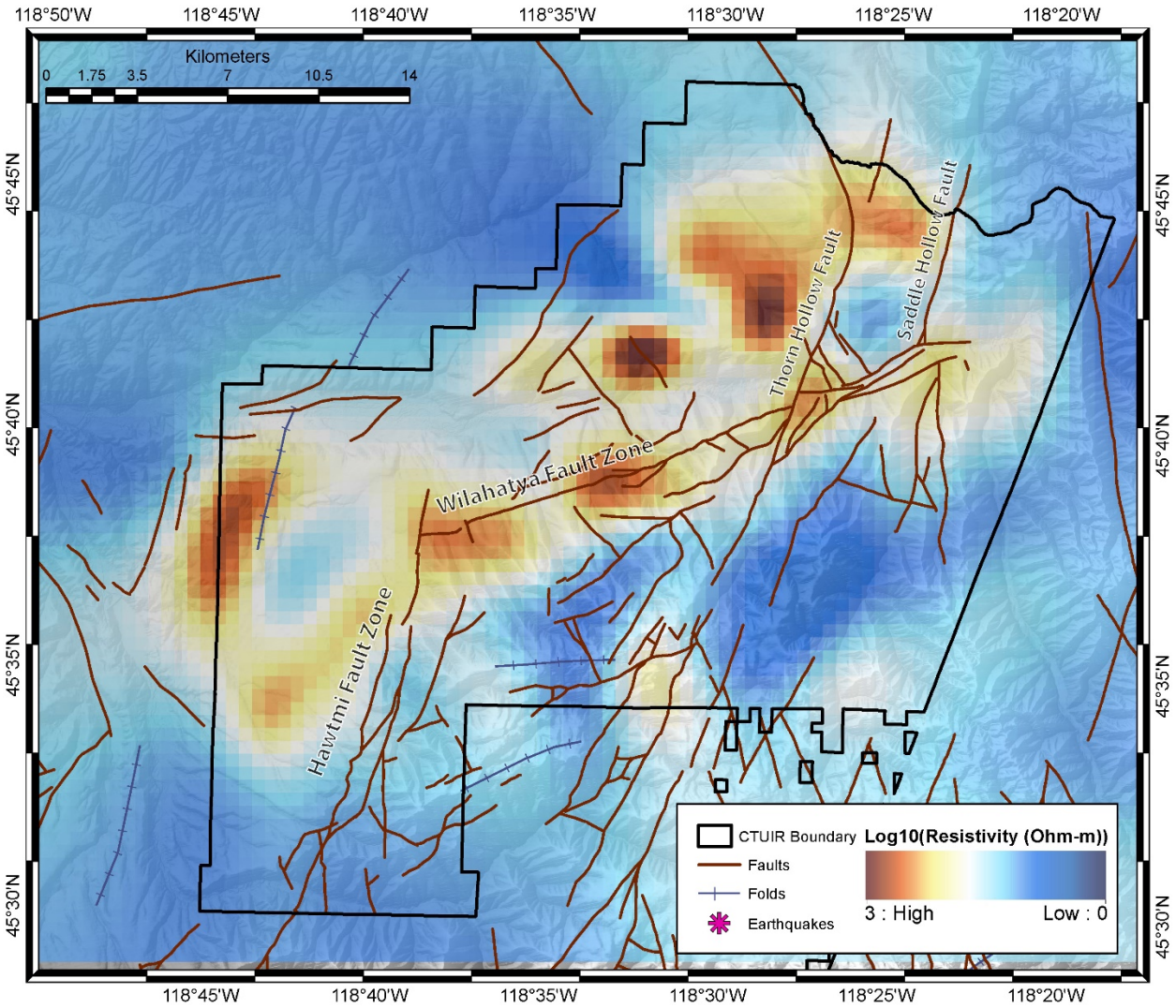

Figure 5. A 2 km depth-slice from MT model illustrating modeled resistive and conductive zones relative to mapped faults (Ferns et al., 2006 and U.S. Geological Survey Quaternary fault database [http://earthquake.usgs.gov/hazards/qfaults]).

6. Discussion

Mapping and modeling of the newly-acquired potential-field data help constrain geology and structures in the mid and upper crust that pertain to both regional and local scales. This structural

characterization is important for identifying potentially significant conduits for the circulation of geothermal fluids and for guiding future exploration that will aid in successfully determining the viability of geothermal resources for development consistent with the policies and priorities of the Confederated Tribes of the Umatilla Indian Reservation. The study area encompasses a region of significant structural complexity that involves the interaction of two major crustal-scale physiographic and geophysical features: the NE-trending KBL (Riddihough et al., 1986 and Raisz, 1945) and the SE-trending OWL (Raisz, 1945; Hooper and Conrey, 1989; Blakely et al., 2011; McCaffrey et al, 2007). The KBL and OWL are manifest on local-scales by numerous sub-parallel structures. The NE to NNE-trending Hawtmi fault, which runs along the eastern margin of the Pendleton basin and along the edge of the Blue Mountains, is the local expression of the KBL in the study area. The NE-trending Thorn Hollow and Saddle Hollow faults along with the ENE-trending Wilahatya fault zone, which appear to be major linkages between the KBL and OWL, run through the region of the UIR and are considered to be important structures controlling geothermal fluid flow. The new potential-field data highlight these features and reveal numerous smaller-scale structures related to these linkages between the KBL and OWL.

Thick sequences of strongly magnetic CRB flows result in pronounced magnetic anomalies that facilitate detailed mapping and modeling of structures in the shallow subsurface. The aeromagnetic data also highlight deeper anomalies, notably a magnetic high situated in the southwestern Blue Mountains, presumably originating from magnetic basement rocks.

A sharp isostatic gravity gradient along the strike of the Hawtmi fault coincides with a break between high-amplitude, short-wavelength magnetic anomalies over the Blue Mountains and lower-amplitude, longer-wavelength anomalies over the Pendleton basin. The correspondence in gravity and magnetic anomalies suggests hundreds of meters (in some regions, exceeding 1km) of down to the west vertical displacement. Modeling suggests that the large gravity low within the southern Pendleton Basin, though partially driven by Quaternary alluvium and loess deposits, is more strongly influenced by a deep sub-CRB sedimentary basin. The modeled depth of this paleobasin suggests significant early-Tertiary vertical motion along the Hawtmi fault. Though the gravity gradient becomes more diffuse to the north, the magnetic gradients indicate that, rather than terminating at the juncture with the Wilahatya fault as indicated by geologic mapping, the Hawtmi fault projects further to the north (Figure 3). North of the Wilahatya, the trend of the Hawtmi fault becomes more northerly until turning north-northwest, paralleling splay structures related to the OWL, before terminating near the Oregon-Washington border.

The large gravity highs within the Blue Mountains to the southwest of the UIR reflect denser basement compositions than those modeled to the northeast. The depth to basement also shallows in the southern portion of the Blue Mountains, where accretionary basement terrain daylights just south of Birch Creek. Modeling reflects shallowing of both basement and overlying pre-CRB sediments in the south.

In the northern portion of the study area, where gravity gradients become subdued, the NNE-trending Thorn Hollow fault, as well as the subparallel Saddle Hollow fault and numerous mapped and unmapped NW-trending intrabasin structures to the west, are still expressed in profiled gravity transects, but are more clearly delineated by gradients in the aeromagnetic data (Figure 3). Another sharp gradient present in the aeromagnetic data, where magnetic lows to the south are juxtaposed against highs to the north, is coincident with the Wilahatya fault. These data

suggest the Wilahatya fault extends further east than previously mapped, approximately 8 km beyond its junction with the Saddle Hollow fault (Figure 3).

Potential-field modeling along profiles running perpendicular to the Hawtmi fault (profiles A, B [not presented in this paper] and C) indicates vertical displacement on the scale of several hundred meters to over a kilometer across the structure. The displacement of the basement along the Hawtmi fault suggests that normal, or possibly oblique dip-slip, motion initiated along the structure during or prior to the late-Paleocene. On the other hand, the model profile across the Wilahatya fault (profile D, model not shown in this paper) indicates little to no vertical motion, suggesting that displacement along this fault has been achieved dominantly via strike-slip motion.

Modeling of CRB flows indicates pervasive vertical-offset along structures running subparallel to the Hawtmi fault in the Blue Mountains and beneath the Pendleton basin. These structures result in a series of horsts and grabens with lateral extents of a few hundred meters to several kilometers and vertical displacement typically in the range of tens to several hundreds of meters. This result is not surprising, as a complex array of faults and their relationship to folding within the Blue Mountains have been described by Ferns et al. (2006) and mapped in previous studies. The depth to which these structures penetrate is difficult to determine, as many of their characteristic anomalies were observed in the aeromagnetic data, which are especially sensitive to offsets in the shallow subsurface. Furthermore, relatively small displacements and the depth to basement contact make the characterization of these faults at depth difficult to ascertain through analysis of gravity data. Inferred faults and numerous subparallel dikes beneath the Pendleton basin observed in the aeromagnetic data provide new insight into previously unknown or merely speculative structures that are obscured by young sediments. The location and trend of intrabasin structures identified in the potential-field mapping and modeling suggest they play a vital role in transferring strain between the KBL and OWL.

When comparing the potential-field models with MT cross sections, conductive regions (warm colors; Figure 5), which may indicate the presence of fluids or clay-rich units, appear within the modeled Herren Formation and basement beneath the Blue Mountains. These conductive zones are capped by a resistive cover that corresponds to CRB flows and the upper portions of pre-CRB sediments. West of the Hawtmi fault, conductive zones deepen and are approximately collocated with the modeled sediment-basement contact and, in some areas, lie almost entirely within the modeled basement. Conductive zone boundaries correspond to the location of major basement structures observed in the potential-field data, which bound shallow modeled horsts and grabens. If conductive zones reflect the presence of fluids, the structures modeled within the basement may be responsible for the vertical transport of these fluids, while fractured basement and porous pre-CRB sediments act as reservoirs. Impermeable horizons within the pre-CRB sediments likely act as caps or barriers to these reservoirs, inhibiting fluid migration except along major structures and contacts.

Potential-field and MT modeling have facilitated the development of a conceptual model for the geothermal framework in the study region (Figure 6), whereby recharge of the geothermal system is provided by meteoric waters that infiltrate deep-seated faults that cut CRB flows within the highlands of the Blue Mountains. Water, heated by interaction with fractured basement rock, rises due to thermal buoyancy. Fluid flow occurs along deep-seated faults and discrete structural intersections along the Wilahatya and Hawtmi fault systems, zones of enhanced permeability.

Geothermal fluids then encounter more permeable layers within the fractured upper basement and lower Herren Formation, accommodating lateral flow of fluids from west to east. Initial analysis of aquatic geochemistry and geothermometry data, obtained as part of the geothermal resource assessment, appear to corroborate this conceptual model.

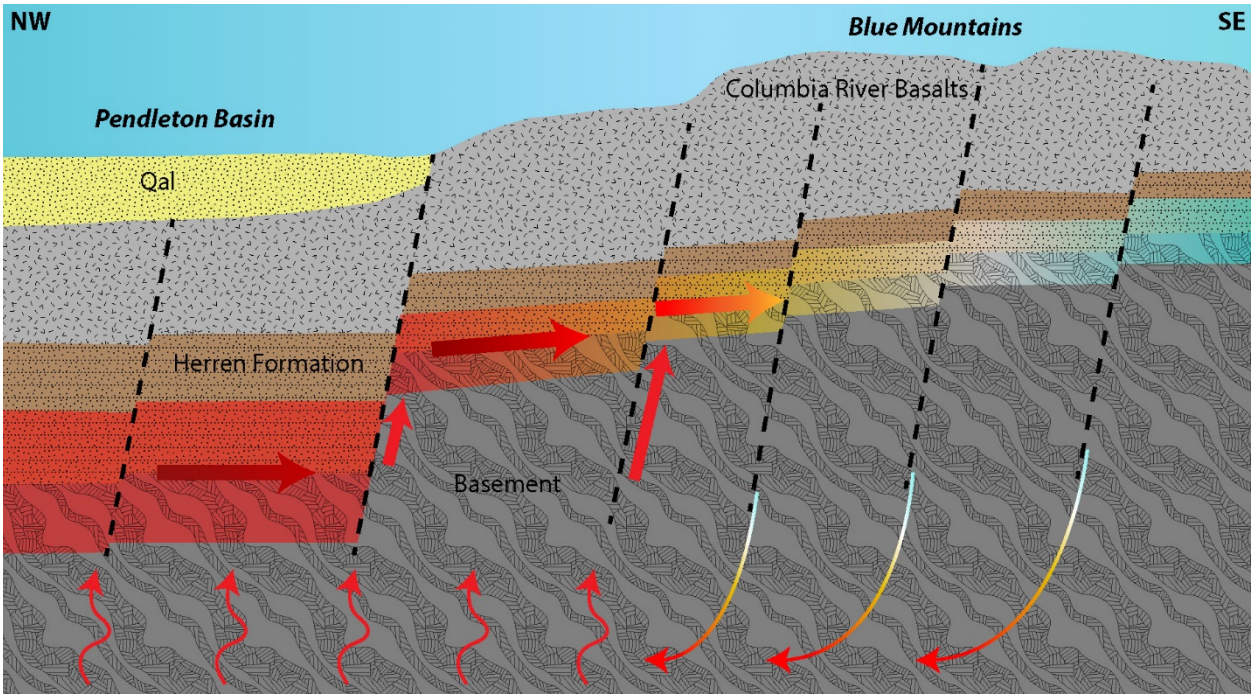

Figure 6. A simple conceptual model of a potential geothermal system on the UIR along a NW-SE profile obliquely crossing the Wilahatya fault zone.

7. Conclusions

Combining prior geologic constraints with new potential-field mapping and modeling helps resolve regional and local geology and faulting in the study area. These data are key to identifying variations in properties of and major compositional boundaries within the basement. The data reveal previously unknown faults, and help further resolve structures that have been previously mapped. The regional trend of these faults highlights their role as linking structures that transfer stress between the KBL and OWL. The detailed geophysical mapping and modeling of these structures, faults and contacts reveal prominent zones of structural complexity (e.g., where major NNE-trending and ENE-trending structures converge), that may correspond to areas of enhanced permeability and fluid migration. Electrically conductive zones identified through MT modeling may represent the presence of fluids or, alternatively, clay-rich units that correspond to primary clay-bearing sediments and/or secondary deposits formed from hydrothermal alteration. South-southwest-dipping conductors, identified through MT modeling, coincide with the deepening of pre-CRB sediments within the Pendleton Basin, inferred from gravity. The dip of the conductor suggests that geothermal fluids may migrate eastward within pre-CRB sediments or along the basement-sediment contact. Conductors are shallowest between the intersections of the Hawtmi and Wilahatya faults and the Thorn Hollow and Wilahatya faults. Focusing further detailed geologic and geophysical data collection and analyses in this region

may aid in better constraining structural geometries and guiding future geothermal exploration activities.

ACKNOWLEDGEMENTS

We thank Drew Siler and Tait Earney for their technical review of the manuscript. We would also like to thank Bruce Chuchel, Zach Palmer and Ben Grober for their help with fieldwork. This work was funded by the Bureau of Indian Affairs (Umatilla Indian Reservation Geothermal Potential Resources Assessment – Phase 1 project), with additional support from the USGS Energy and Earthquake Hazards Programs.

REFERENCES

Blakely, R. J., and R. W. Simpson, 1986, Approximating edges of source bodies from magnetic and gravity anomalies, Geophysics, 51, 1494–1498.

Blakely, R. J., and G.G. Connard, 1989. Crustal studies using magnetic data, in Pakiser, L.C., and Mooney, W.D., eds., Geophysical framework of the continental United States, Geological Society of America Memoir 172, 45-60.

Blakely, R. J., 1995. Potential theory in gravity and magnetic applications: New York, Cambridge University Press, 441 p.

Blakely, R.J., Sherrod, B.L., Weaver, C.S., Wells, R.E., Rohay, A.C., Barnett, E.A., and Knepprath, N.E., 2011, Connecting the Yakima fold and thrust belt to active faults in the Puget Lowland, Washington: Journal of Geophysical Research, v. 116, B07105, doi:10.1029/2010JB008091.

Blakely R.J, B.L. Sherrod, C.S. Weaver, R.E. Wells, and A.C. Rohay, 2014. The Wallula fault and tectonic framework of south-central Washington, as interpreted from magnetic and gravity anomalies, Tectonophysics, v. 624-625, p. 32-45, doi:10.1016/j.tecto.2013.11.006.

Chave, A.D., and D.J. Thomson, 2004. Bounded influence magnetotelluric response function estimation. Geophys. J. Int., 157, 988–1006.

Cogné, J. P., 2003, PaleoMac: A Macintosh™ application for treating paleomagnetic data and making plate reconstructions, Geochemistry, Geophysics, Geosystems, 4(1), n/a-n/a, doi: 10.1029/2001GC000227.

Egbert, G. D., and A. Kelbert, 2012. Computational recipes for electromagnetic inverse problems. Geophys. J. Int., 189, 251–267.

Ferns, M.L., V.S. McConnell, and K. Ely, 2004. Field trip guide to the geology of the Umatilla River Basin, Oregon: Oregon Department of Geology and Mineral Industries Open-File Report O-04-23, 1 cd.

Ferns, M.L., J.D. McClaughry, V.S. McConnell, and I.P. Madin, 2006. Geology of the Umatilla and parts of the middle Columbia - Lake Wallula basins, Gilliam, Morrow, Umatilla, and Union Counties, Oregon: Oregon Department of Geology and Mineral Industries, Unpublished manuscript.

Fisher, R., 1953, Dispersion on a Sphere, Proceedings of the Royal Society of London A: Mathematical, Physical and Engineering Sciences, 217(1130), 295-305, doi: 10.1098/rspa.1953.0064.

Herrera, N.B., K. Ely, S. Mehta, A.J. Stonewall, J.C. Risley, S.R. Hinkle and T.D. Conlon, 2017. Hydrogeologic framework and selected components of the groundwater budget for the upper Umatilla River Basin, Oregon (No. 2017-5020). US Geological Survey.

Kelbert, A., N.M. Meqbel, G.D. Egbert, & K. Tandon, 2014, ModEM: a modular system for inversion of electromagnetic geophysical data. Computer Geoscience, 66, 40–53.

Kirschvink, J. L., 1980, The least-squares line and plane and the analysis of palaeomagnetic data, Geophysical Journal International, 62(3), 699-718, doi: 10.1111/j.1365-246X.1980.tb02601.x.

Kirschvink, J. L., R. E. Kopp, T. D. Raub, C. T. Baumgartner, and J. W. Holt, 2008, Rapid, precise, and high-sensitivity acquisition of paleomagnetic and rock-magnetic data: Development of a low-noise automatic sample changing system for superconducting rock magnetometers, Geochemistry, Geophysics, Geosystems, 9, Q05Y01, doi:10.1029/2007GC001856

Krieger, L., and J.R. Peacock, 2014. MTpy: a Python toolbox for magnetotellurics. Computers & Geoscience, 72, 167–175.

McCaffrey, R., A.I. Qamar, R.W. King, R. Wells, G. Khazaradze, C.A. Williams, C.W. Stevens, J.J. Vollick, and P.C. Zwick, 2007. Fault locking, block rotation and crustal deformation in the Pacific Northwest. Geophysical Journal International, 169(3), pp.1315-1340.

McFadden, P. L., and M.W. McElhinny, 1988, The combined analysis of remagnetization circles and direct observations in palaeomagnetism, Earth and Planetary Science Letters, 87(1–2), 161-172, doi: http://dx.doi.org/10.1016/0012-821X(88)90072-6.

Phillips, J.D., 2001, Designing matched bandpass and azimuthal filters for the separation of potential-field anomalies by source region and source type: Extended abstract, ASEG 15th Geophysical Conference and Exhibition, August 2001, Brisbane, Australia.

Raisz, E., 1945, The Olympic-Wallowa lineament. In Proc. Sess, No. 1364, pp. 42-43.

Reidel, S.P., Campbell, N.P., Fecht, K.R., and Lindsey, K.A., 1994, Cenozoic structure and stratigraphy of south-central Washington, in Regional Geology of Washington State: Washington Division of Geology and Earth Resources Bulletin, v. 80, p. 159-180.

Riddihough, R., C. Finn, and R. Couch, 1986, Klamath-Blue Mountain lineament, Oregon, Geology, 14, 528–531.

Schwartz, J.J., A.W. Snoke, C.D. Frost, C.G. Barnes, L.P. Gromet and K. Johnson, 2010. Analysis of the Wallowa-Baker terrane boundary: Implications for tectonic accretion in the Blue Mountains province, northeastern Oregon. GSA Bulletin, 122(3/4), 517–536.

Talwani, M., J. L. Worzel, and M. Lisman, 1959, Rapid gravity computation of two dimensional bodies with application to Mendocino submarine fracture zone, J. Geophys. Res., 64, 95–137.

U.S. Geological Survey, 2006, Quaternary fault and fold database for the United States, accessed June 16, 2016, from USGS web site: http//earthquake.usgs.gov/hazards/qfaults/

Vallier, T.L., 1998, Islands and Rapids: A geologic story of Hells Canyon: Lewiston, Idaho, Confluence Press, Lewis-Clark State College, 151 p.